Tibi, R., Bock, G., Xia, Y., Baumbach, M., Grosser, H., Milkereit, C., Karakisa, S., Zünbül, S., Kind, R., Zschau, J. (2001): Rupture processes of the 1999 August 17 Izmit and November 12, Düzce (Turkey) earthquakes. - Geophysical Journal International, 144, 2, pp. F1—F7.

DOI: http://doi.org/10.1046/j.1365-246x.2001.00360.x

Geophys. J. Int. (2001) **144,** F1–F7

FAST-TRACK PAPER

Rupture processes of the 1999 August 17 Izmit and November 12 Düzce (Turkey) earthquakes

R. Tibi,[1,*] G. Bock,[1] Y. Xia,[1] M. Baumbach,[1] H. Grosser,[1] C. Milkereit,[1] S. Karakisa,[2] S. Zünbül,[2] R. Kind[1] and J. Zschau[1]

[1] *GeoForschungsZentrum Potsdam, Telegrafenberg,* 14473 *Potsdam, Germany. E-mail: bock@gfz-potsdam.de*
[2] *General Directorate of Disaster Affairs, Earthquake Research Department, Eskisehir Yolu–Lodumlu* 06530, *Ankara, Turkey*

Accepted 2000 November 2. Received 2000 September 11; in original form 2000 May 31

SUMMARY

We derive the rupture history of the 1999 August 17 Izmit ($M_w = 7.4$) and 1999 November 12 Düzce ($M_w = 7.1$) earthquakes in Turkey from teleseismic body waves using broad-band data of the Global Seismograph Network, aftershock locations and mapped surface breaks. The centroid solutions indicate strike-slip mechanisms for both events. The Izmit earthquake was characterized by rupture propagating predominantly eastwards. It consisted of a main rupture lasting about 25 s followed within 1 min by two more events of $M_w = 6.9$ and $M_w = 7.0$. With the teleseismic data, we could not resolve the westward extent of rupture into the Marmara Sea. However, an upper bound of the seismic moment release west of the epicentre of the Izmit event is estimated to be 1.9×10^{19} N m. The Düzce earthquake lasted about 14 s and was characterized by a bilateral mode of rupture, in excellent agreement with mapped surface breaks and aftershock locations.

Key words: body waves, earthquake source mechanism, North Anatolian fault, seismic moment, Turkey, waveform analysis.

1 INTRODUCTION

On 1999 August 17 a large, devastating earthquake ($M_w = 7.4$) occurred in northwestern Turkey near the port city of Izmit, killing more than 16 000 people. The event ruptured a segment of the North Anatolian Fault (NAF) that was previously identified as a seismic gap (Toksöz *et al.* 1979). About 3 months later, on 1999 November 12, a second devastating earthquake of $M_w = 7.1$ nucleated near Düzce, about 120 km east of Izmit.

We employed the method of Nábělek (1984) to deduce source parameters of these earthquakes from teleseismic broad-band seismograms provided by the IRIS Data Management Center (DMC). The method applies waveform modelling of teleseismic *P* and *SH* waves to invert for source model parameters in a least-squares sense. Teleseismic *P* and *SH* waveforms have been deconvolved to ground displacement and band-pass filtered at 0.01–0.1 Hz. The IASP91 model was used to model crustal structure in the source region, while a half-space was assumed under the receivers. Source models studied included centroid models, unilaterally and bilaterally moving point sources, and models of several point sources. For each point source, the far-field source time function is parametrized by a series of triangular-shaped pulses of 1 s length.

Aftershock locations were obtained with the HYPO71 hypocentre location program using manually picked arrival times of *P* and *S* waves of the SABO (Sapanca–Bolu) network. The network consists of 15 short-period stations covering the area between the Izmit and Düzce events (Fig. 1a). The geometry of the network allows reliable locations of aftershocks to be obtained within the SABO network, but location accuracy deteriorates for events outside the network.

The NAF forms the northern rim of the Anatolian subplate, which moves about 2 cm yr^{-1} westwards relative to Eurasia (Jackson & McKenzie 1988; Argus *et al.* 1989; Armijo *et al.* 1999). The strike-slip focal mechanisms of both the Izmit and Dücze events are consistent with this tectonic setting (Table 1).

2 THE IZMIT EARTHQUAKE

The seismic moment, $M_0 = 1.47 \times 10^{20}$ N m, for the centroid model (Table 1) agrees well with estimates of 1.4×10^{20} N m published by the USGS and Toksöz *et al.* (1999). The centroid is located approximately 30 km east of the epicentre (Fig. 1a)

* Now at: Department of Earth and Planetary Sciences, Washington University, St. Louis, MO 63130, USA.

Table 1. Source parameters of the centroid solutions determined in this study.

	Strike (°)	Dip (°)	Rake (°)	M_0 (N m)
1999 August 17 Izmit	270	83	181	1.47×10^{20}
1999 November 12 Düzce	263	62	184	0.47×10^{20}

in the area where maximum surface ruptures were observed (Fig. 3).

The model of a propagating point source was used to approximate unilateral rupture of constant velocity V_r. The inversion yields an eastward rupture in the direction 85°E ± 10° propagating with a velocity $V_r = 4.5 \pm 1.5$ km s^{-1}. The best value of 4.5 km s^{-1} could indicate supershear rupture velocity, but the estimated standard error is large. A very high rupture velocity of 4.7 km s^{-1} is inferred from a near-field strong-motion recording obtained at a station near Adapazari, about 40 km E of the epicentre (Ellsworth & Celebi 1999). Using the best-fitting value for V_r and its lower bound, we inferred the moment distribution of the main rupture episode and compared it with aftershock locations (Figs 1b and c). Aftershocks located by the SABO network fall into two clusters centred about 50 and 90 km east of the epicentre. Aftershocks to the west are not well located because they are outside the network's aperture.

While the centroid model and a model of an eastward propagating point source are sufficient to explain the rupture

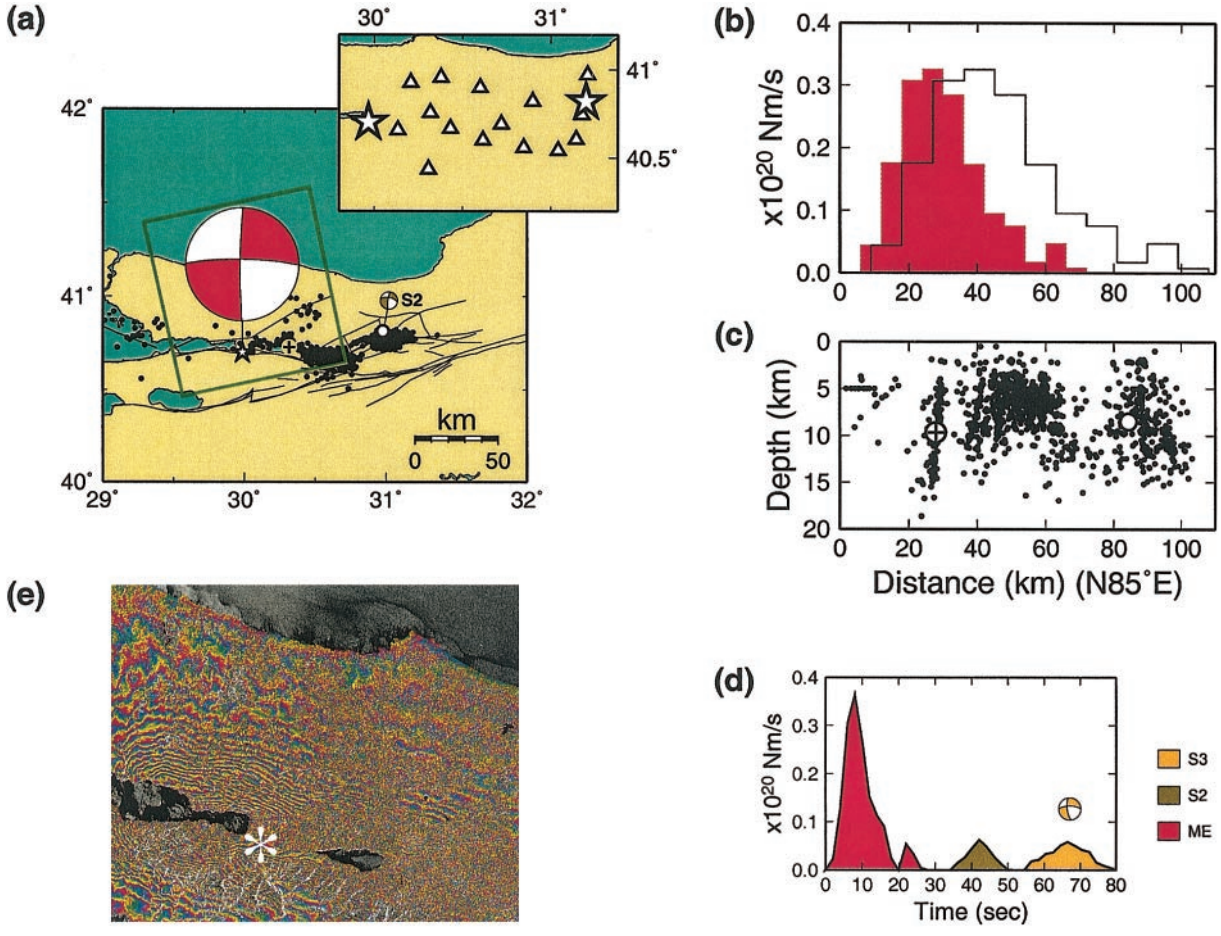

Figure 1. (a) Map of the epicentral area of the Izmit earthquake showing the epicentre of the main shock (star) at 40.702°N, 29.987°E (USGS). Circle denotes event S2. Cross is the centroid location at 40.729°N, 30.316°E inferred in this study. Dots are aftershock locations from SABO network. The focal mechanisms of the main rupture, ME, and event S2 are lower-hemisphere projections whose areas are proportional to the seismic moment. Lines indicate mapped faults. The inset map shows the station distribution of the local SABO network, and the epicentres (stars) of the Izmit and Düzce earthquakes. (b) Moment distribution for the main rupture episode inferred for a propagating point source model. The distance from the nucleation point is calculated for the best-fitting rupture velocity, $V_r = 4.5$ km s^{-1} (line), and for $V_r = 3.0$ km s^{-1} (shaded). (c) Vertical cross-section showing locations of aftershocks, the centroid (cross) and event S2 (circle). (d) Source time function of the main rupture episode ME and the events S2 and S3, which occurred about 35 and 55 s after the main rupture initiation, respectively. Also represented is the fault plane solution for S3. (e) Apparent coseismic deformation pattern caused by the Izmit earthquake for the area bounded by the green rectangle shown in (a) derived from SAR interferometry. White asterisk represents the epicentre of the Izmit event. The interferogram was generated by using data pairs of ERS-1 (the first European Remote Sensing Satellite), orbit 42229 frame 0819 date 08/12/1999 and orbit 42730 frame 0819 date 09/16/1999. Each fringe (colour cycle) in this figure corresponds to a ground displacement of 2.8 cm in the satellite's viewing direction (slant range). In the interferogram, 24 fringes can be observed on both sides of the NAF, indicating a symmetrical displacement. The 24 fringes represent a slip of 67.2 cm in the slant range or 1.72 m in the ground direction. Thus, the relative offset along the E–W-trending fault, extending about 70 km to the west of the inferred position of the epicentre, is 3.44 m.

process in the first 25 s, some details of the *P*-wave coda in the first 60 s could not be matched. Satisfactory waveform fits (Fig. 2) were obtained with a model of three non-propagating point sources (Fig. 1d and Table 2). Two major events termed S2 and S3 followed the main rupture episode (ME) within 1 min (Fig. 1d). S2 is located 80 ± 10 km to the east of the hypocentre, placing it in the aftershock area near 31°E (Fig. 1a). It was not possible to constrain the location of S3 with the same precision as that of S2; however, S3 must have also been located east of the rupture initiation. The main event, ME, lasted approximately 25 s and its associated moment release was 1.6×10^{20} N m, slightly higher than the centroid moment. This corresponds to $M_w = 7.4$ using the relationship between seismic moment and moment magnitude (Kanamori 1977). The moment magnitudes of events S2 and S3 are $M_w = 6.9$ and $M_w = 7.0$, respectively.

The inversion results indicate a slight change in focal mechanism from ME to S2 and S3 (Table 2). The E–W-trending nodal planes of S2 and S3 dip less steeply than the E–W nodal plane of ME ($83° \pm 1°$), and their dip angles are close to those observed for the Düzce earthquake (62°). The results suggest that ME and S2 were associated with different fault segments of the NAF. The main event terminated about 60–80 km east of rupture initiation, possibly as a result of a change in the fault

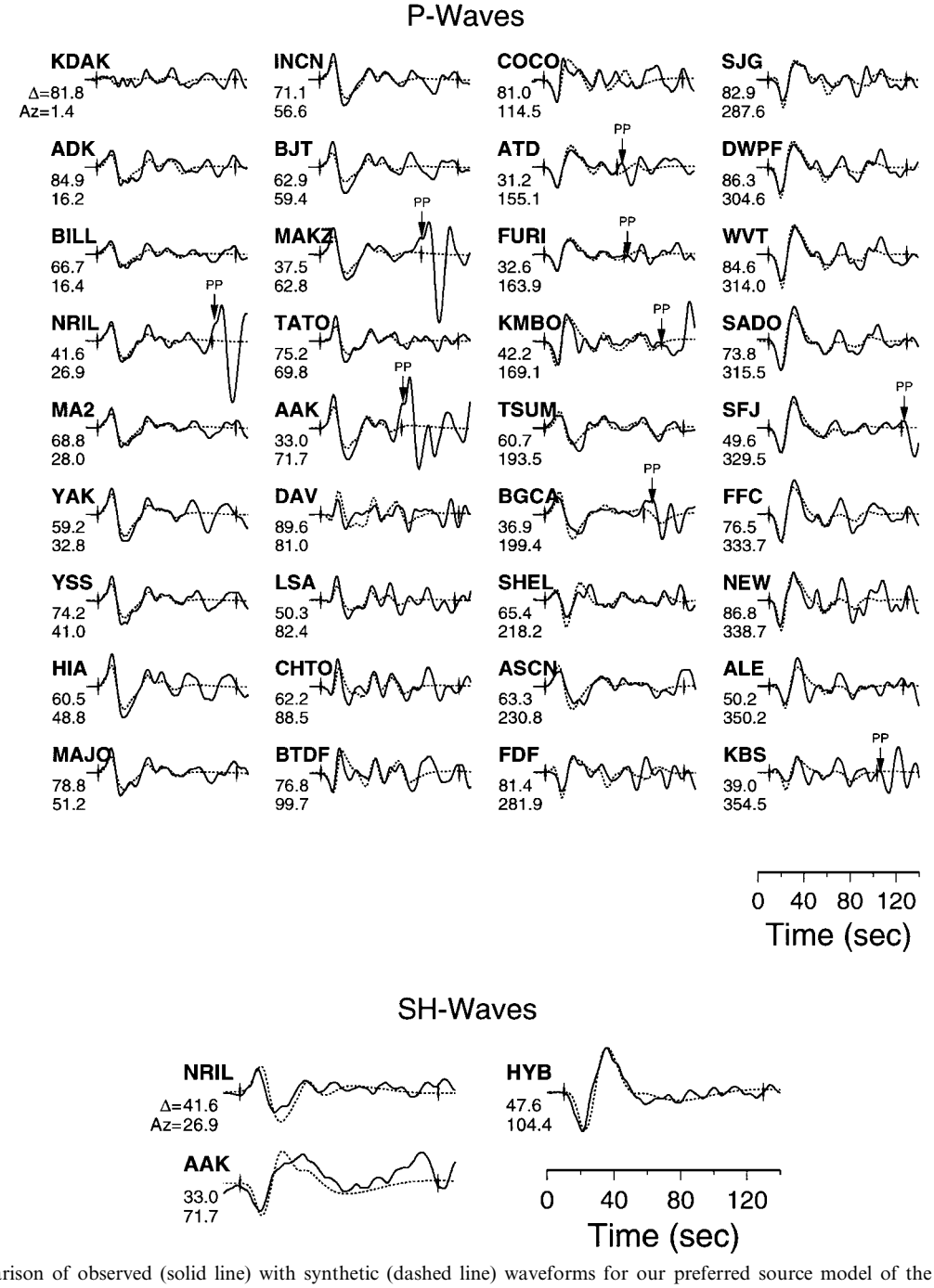

Figure 2. Comparison of observed (solid line) with synthetic (dashed line) waveforms for our preferred source model of the Izmit earthquake. Epicentral distance and azimuth are given below the station code.

Table 2. Focal mechanisms (strike, dip and rake of rupture plane), seismic moments and their standard deviations for the subevents of the Izmit and Düzce earthquakes. The orientations of the rupture planes for subevents PE and PW of the Düzce event were held fixed in the inversion (indicated by asterisks).

	Strike (°)	Dip (°)	Rake (°)	M_0 ($\times 10^{20}$ N m)
Izmit event				
Main rupture ME	271±1	83±1	183±1	1.56±0.04
S2	283±7	60±9	191±4	0.24±0.01
S3	270±5	69±4	201±5	0.38±0.02
Düzce event				
PE	263*	62*	184*	0.36±0.01
PW	263*	62*	184*	0.18±0.02

geometry (King & Nábělek 1985). The S2 event was located on a northerly strand of the NAF, while the main segment of the NAF located to the south of S2 remained aseismic. S2 represents an earthquake that was probably triggered by stress distribution of the Izmit earthquake. The extent of mapped surface breaks and the slip distribution (Fig. 3) suggest that S2 and its associated aftershocks terminated in the east at about 31°E. This location may represent a barrier that prevented rupture propagation further east, towards the region of the Düzce earthquake. The same barrier marks the westernmost end of the Düzce earthquake.

The coseismic deformation of the Izmit earthquake has been independently determined by means of interferometric synthetic aperture radar (InSAR) techniques (Fig. 1e). The phase difference of two SAR single-look images provides a valuable source of geometric information, and changes in topography and deformation can be derived from images of successive acquisitions. Using acquisitions on August 12 and September 16 1999, the interferogram shown in Fig. 1(e) was generated. A westward component of rupture is indicated by the InSAR results that were modelled by 1.5 to 3 m displacement along an E–W-trending fault extending about 60–70 km to the west of the inferred epicentre position, well into the Marmara Sea (see also Wright *et al.* 1999). Furthermore, the distribution of aftershocks determined by Honkura *et al.* (2000) indicates that rupture might have extended as far west as 29.1°E. GPS data, however, do not require westward rupture into the Marmara Sea (Reilinger *et al.* 1999). Surface slips in the Hersek area (Fig. 3) were difficult to evaluate; they are probably of the order of only a few centimetres. Therefore, the extent of surface breaks to the west of the epicentre, shown in Fig. 3 as a dashed red line with a question mark, must be regarded as uncertain. Models with a component of westward rupture propagation

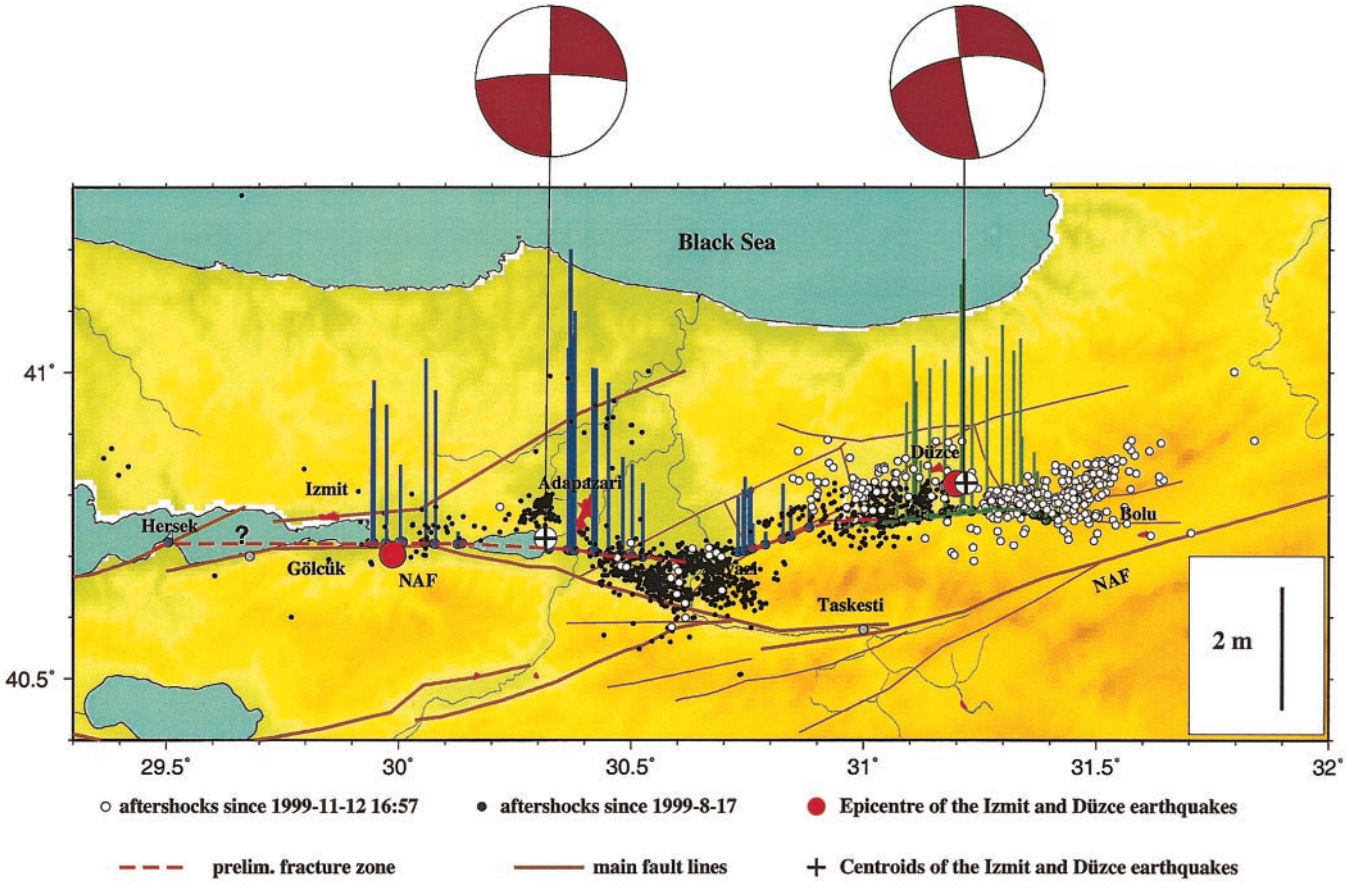

Figure 3. Map showing aftershocks (located by SABONET) of the Izmit (black circles) and Düzce events (white circles). Epicentres of the Izmit and Düzce events are plotted as red dots and their respective centroid locations as crosses. The centroid mechanisms for the main Izmit and Düzce events are shown above the map. Mapped surface ruptures of the Izmit and Düzce earthquakes (scale in the lower right-hand corner) are represented by red and green dashed lines, respectively. The red dashed lines through Lake Sapanca and the Marmara Sea have been interpolated between observations made on land. The extension of surface breaks to the west of the Izmit epicentre is uncertain.

did not provide significantly improved waveform fits over our best model of Table 2. We estimated an upper bound of the seismic moment release west of the Izmit epicentre to be 1.9×10^{19} N m, corresponding to an $M_w = 6.8$ event. The associated average slip would have been 1 m over a fault area of 60 km × 10 km.

3 THE DÜZCE EARTHQUAKE

The Düzce earthquake nucleated east of the S2 event of 1999 August 17. The centroid estimated by body wave modelling (Fig. 3) is only 2 km east of the epicentre, suggesting no clear directivity of rupture. Using a model of a unilaterally propagating point source, a directivity towards N75°E is indicated, which is nearly parallel to one of the nodal planes of the centroid mechanism (Table 1). The inferred velocity of 1 km s^{-1} for the propagating point source, however, is very low and speaks against unilateral rupture as a realistic source model.

The location of the centroid in the immediate vicinity of the hypocentre has two possible causes: the rupture area was either extremely compact or rupture propagated bilaterally from the hypocentre. The first model implies that the rupture area might not exceed approximately 10 km × 10 km. This appears to be most unlikely in view of the aftershock distribution and the mapped slip distribution at the surface (Fig. 3). Therefore, the model of a very compact rupture area for the Düzce earthquake is discarded.

Bilateral rupture is supported by several observations. Aftershocks (Fig. 3) are located east and west of the epicentre. Surface breaks have been mapped over approximately 43 km in an E–W direction, as marked by the dashed green line in Fig. 3, and extending bilaterally from the epicentre. For a purely symmetrical bilateral rupture the centroid would coincide with the epicentral location. The rupture velocity of 1 km s^{-1} inferred from the model of unilateral rupture underestimates the rupture velocity for bilateral rupture by a factor of approximately two (Ihmle 1998). Following Ihmle (1998), we assume that during the Düzce earthquake rupture propagated bilaterally at about 2 km s^{-1} from the nucleation point.

Our preferred source model (Fig. 4 and Table 2) approximates a bilateral rupture propagating N75°E (PE) and S75°W (PW) with $V_r = 2$ km s^{-1}. Observed and theoretical seismograms calculated for the model are compared in Fig. 5. The fits are excellent. The moment distribution shown in Fig. 4(b) indicates that rupture propagated about 25 km to the east and 30 km to the west, in agreement with the length of the aftershock area. The eastward-propagating rupture PE released a seismic moment of 0.36×10^{20} N m, twice as much as that released by PW to the west (0.18×10^{20} N m). Similarly, aftershock activity is higher to the east than to the west of the nucleation point (Fig. 4b). The source time function (Fig. 4a) is characterized by two peaks at about 3 and 8 s. The model not only explains the absence of directivity effects at stations in the easterly and westerly azimuths, but it also provides a good match of the *P*-wave pulse broadening observed at stations in the south and shortening observed in the north (Fig. 5). It can be shown by synthetic seismograms that these observed differences in pulse duration are caused by superposition of *P* and the depth phases *pP* and *sP*, and not by rupture directivity from south to north.

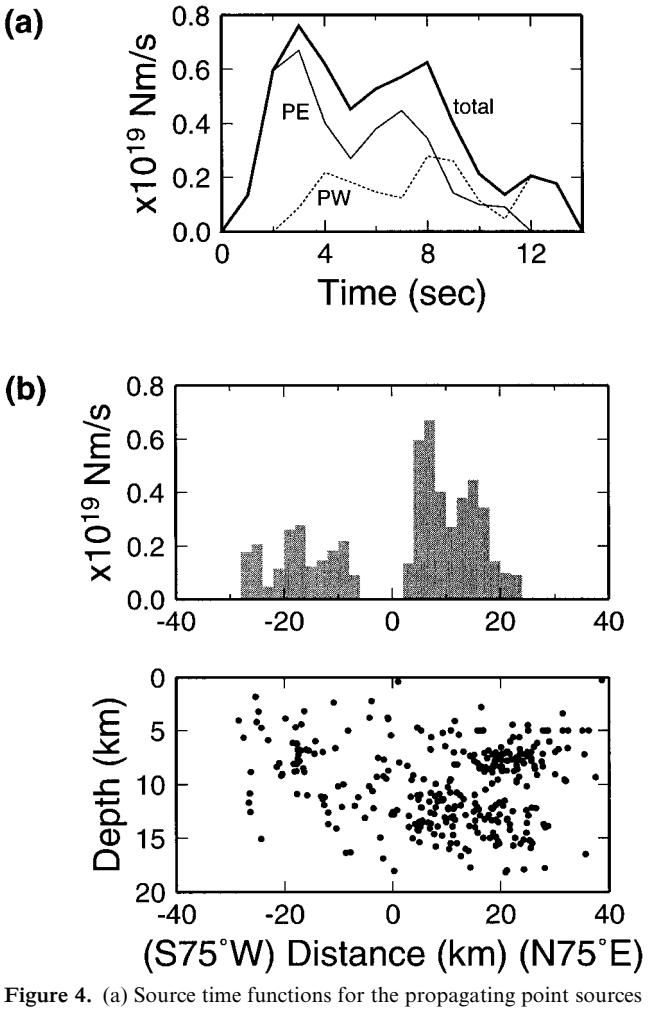

Figure 4. (a) Source time functions for the propagating point sources PE and PW used to model the bilateral rupture of the Düzce event, and the total PE + PW. (b) Moment distribution (top) inferred for the model of two point sources propagating bilaterally towards N75°E and S75°W with a velocity of 2 km s^{-1}. The vertical cross-section (bottom) shows aftershock locations.

4 CONCLUSIONS

The main results of the body wave inversion are provided in Table 1 for the centroid model and in Table 2 for models of several point sources. Other derived parameters are summarized in Table 3. The fault areas are based on directivity analysis and aftershock distribution. Static stress drops have been estimated using the relationship for a rectangular fault (Lay & Wallace 1995) and considering the free-surface effect. The average displacement D has been derived using $D = M_0/\mu S$, where $\mu = 31$ GPa is the rigidity and $S = LW$ is the fault area.

Table 3. Inferred source parameters of the Izmit and Düzce earthquakes.

	Izmit	Düzce
Rupture velocity (km s^{-1})	4.5?	2
Fault area $L \times W$ (km^2)	100 × 20	55 × 20
Static stress drop (MPa)	4	2
Average fault slip (m)	2.5	1.6

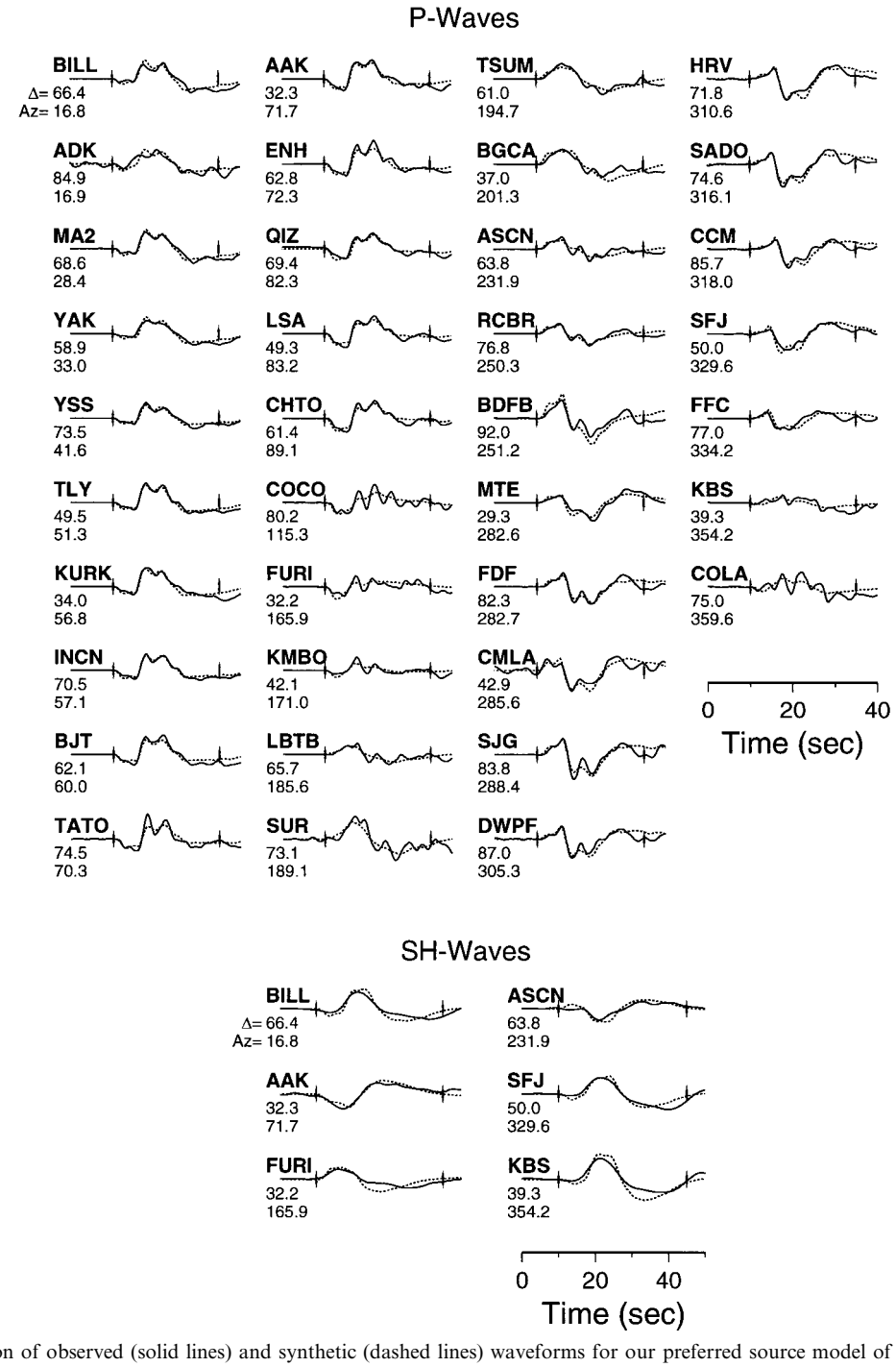

Figure 5. Comparison of observed (solid lines) and synthetic (dashed lines) waveforms for our preferred source model of the Düzce earthquake. Epicentral distance and azimuth are given below the station code. Teleseismic *P* and *SH* waveforms have been deconvolved to ground displacement and high-pass filtered at 0.01 Hz.

Rupture in the Izmit earthquake extended from the epicentre located at 40.702°N, 29.987°E about 100 km to the east, in agreement with the fault length inferred by Toksöz *et al.* (1999). A westward directivity of rupture cannot be resolved from the teleseismic data we used; a value of 0.19×10^{20} N m represents an upper bound of moment released to the west of the epicentre. Within 1 min of the main rupture two more events occurred with moments of 0.24×10^{20} and 0.38×10^{20} N m. The first event, S2, was located approximately 80 km to the east of the hypocentre, within the easternmost area of aftershocks observed after the Izmit earthquake. The main Izmit event and S2 represent earthquakes on different strands of the North Anatolian fault system, as indicated by the aftershock distribution and mapped surface faults (Fig. 3). The area of the S2 event seemed to be a barrier to further eastward rupture propagation, and it marks the westernmost extent of rupture in the Düzce earthquake. One possible explanation is that this barrier marks the position of a change in fault morphology. Another possibility is that S2 and the Düzce earthquake took place on different fault segments that were activated at different

times. The latter model is supported by the aftershock distribution observed after the Düzce earthquake, which is offset to the north by about 15 km relative to events prior to it (Milkereit *et al.* 2000).

ACKNOWLEDGMENTS

Financial funds for this research were provided by GeoForschungsZentrum Potsdam (GFZ), the Deutsche Forschungsgemeinschaft (grant Ri 607/7-1) and the DG XII of the EU (project ENV4-CT96-0282). The SABO network in northwestern Turkey is jointly operated by GFZ and the Earthquake Research Department of the General Directorate of Disaster Affairs at Ankara. We thank the operators of the IRIS, GEOSCOPE and GEOFON networks, who made available data immediately after the events, ESA (European Space Agency) and DLR (Deutsches Zentrum für Luft- und Raumfahrt) for their support and providing the radar data, Ünal Dikmen, Erwin Günther and Wolfgang Welle for contributing data on surface ruptures, and Bernd Schurr and Gero Michel for reading the manuscript. We also thank Michel Bouchon and an anonymous referee for their valuable suggestions on the manuscript. Most figures were generated using the GMT software (Wessel & Smith 1991).

REFERENCES

Argus, D.F., Gordon, R.G., DeMets, C. & Stein, S., 1989. Closure of the Africa-Eurasia-North America plate motion circuit and tectonics of the Gloria fault, *J. geophys. Res.,* **94,** 5585–5602.

Armijo, R., Meyer, B., Hubert, A. & Barka, A.A., 1999. Westward propagation of the North Anatolian fault into the northern Aegean: timing and kinematics, *Geology,* **27,** 267–270.

Ellsworth, W.L. & Celebi, M., 1999. Near field displacement time histories of the M7.4 Kocaeli (Izmit), Turkey, earthquake of August 17, 1999, *EOS, Trans. Am. geophys. Un.,* **80,** F648.

Honkura, Y., *et al.*, 2000. Preliminary results of multidisciplinary observations before, during and after the Kocaeli (Izmit) earthquake in the western part of the North Anatolian Fault Zone, *Earth Planets Space,* **52,** 293–298.

Ihmle, P.F., 1998. On the interpretation of subevents in teleseismic waveforms: the 1994 Bolivia deep earthquake revisited, *J. geophys. Res.,* **103,** 17 919–17 932.

Jackson, J.A. & McKenzie, D., 1988. The relationship between plate motions and seismic moment tensors, and the rate of active deformation in the Mediterranean and Middle East, *Geophys. J. Int.,* **93,** 45–73.

Kanamori, H., 1977. The energy release in great earthquakes, *J. geophys. Res.,* **82,** 2981–2987.

King, G. & Nábělek, J.L., 1985. Role of fault bends in the initiation and termination of earthquake rupture, *Science,* **228,** 984–987.

Lay, T. & Wallace, T.C., 1995. *Modern Global Seismology,* Academic Press, San Diego, CA.

Milkereit, C., *et al.*, 2000. Preliminary aftershock analysis of the Mw = 7.4 Izmit and Mw = 7.1 Düzce earthquake in western Turkey, *Proc. AGU Fall Mtng on the August 17, 1999, Izmit, Turkey,* pp. 179–187, ed. Barka, A., Istanbul Technical University.

Nábělek, J.L., 1984. Determination of earthquake source parameters from inversion of body waves, *PhD thesis,* MIT, Cambridge, MA.

Reilinger, R., *et al.*, 1999. Coseismic slip for the August 17, 1999, M = 7.4, Izmit, Turkey earthquake from surface faulting and GPS measurements, *EOS, Trans. Am. geophys. Un.,* **80,** F649.

Toksöz, M.N., Shakal, A.F. & Michael, A.J., 1979. Space-time migration of earthquakes along the North Anatolian Fault zone and seismic gaps, *Pageoph,* **117,** 1258–1270.

Toksöz, M.N., Reilinger, R.E., Doll, C.D., Barka, A.A. & Yalcin, N., 1999. Izmit (Turkey) earthquake of 17 August 1999: first report, *Seism. Res. Lett.,* **70,** 669–679.

Wessel, P. & Smith, W.H.F., 1991. Free software helps map and display data, *EOS, Trans. Am. geophys. Un.,* **72,** 445–446.

Wright, T.J., England, P.C., Fielding, E.J., Haynes, M. & Parsons, B.E., 1999. Source parameters of the 17 August 1999 Izmit earthquake from SAR interferometry, *EOS, Trans. Am. geophys. Un.,* **80,** F671.